

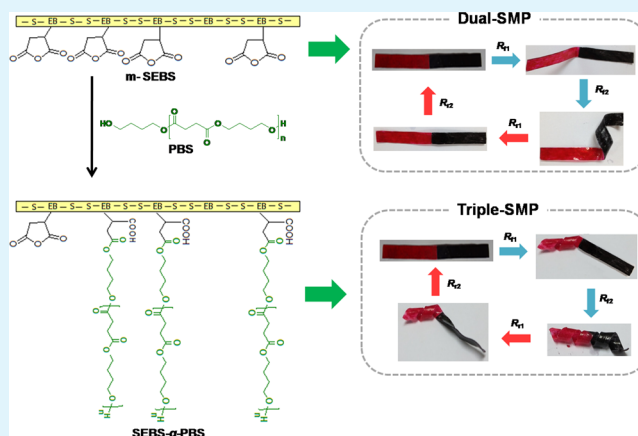
# “Grafting to” as a Novel and Simple Approach for Triple-Shape Memory Polymers

Kanitporn Suchao-in<sup>†</sup> and Suwabun Chirachanchai<sup>\*,†,‡</sup>

<sup>†</sup>The Petroleum and Petrochemical College and <sup>‡</sup>Center for Petroleum, Petrochemicals, and Advanced Materials, Chulalongkorn University, Bangkok, 10330, Thailand

## S Supporting Information

**ABSTRACT:** Maleated-polystyrene-*b*-poly(ethylene-co-butylene)-*b*-polystyrene (m-SEBS) is a block copolymer with two melting temperatures belonging to soft poly(ethylene-co-butylene) (EB) and hard polystyrene (PS) segments. As EB segments contain anhydride reactive groups, this allows grafting polybutylene succinate (PBS) as another soft segment to m-SEBS backbone to obtain triple-shape memory polymers based on two transition temperatures, i.e.,  $T_m$  values of EB (at 55–65 °C) and PBS (at 105–115 °C). The present work shows a novel and simple approach of “grafting to” to develop triple-shape memory polymers.



**KEYWORDS:** triple-shape memory, SEBS, polybutylene succinate, grafting to

## INTRODUCTION

Shape memory polymers (SMPs) are smart materials that can be fixed into the temporary shapes and recovered to their original shape by external stimuli, so-called shape memory effect (SME).<sup>1–3</sup> In fact, SME is generic features of polymeric materials under a combination of polymer morphology and specific polymer processing as referred to polymer functionalization.<sup>4–6</sup> At the right programming condition, the key mechanisms, which are the chain mobility change and the new phase formation, initiate SME resulting in the temporary shape.<sup>7–13</sup>

Thermo-responsive SMPs are good examples which the transition temperature ( $T_{\text{tran}}$ ) and the consequent fixing up polymer network can be induced either by heating up or cooling down.<sup>14,15</sup> It is important to note that  $T_{\text{tran}}$  can be glass transition temperature ( $T_g$ ), melting temperature ( $T_m$ ), and liquid crystallization temperature ( $T_{cl}$ ).<sup>3</sup> On the viewpoint of polymer structure, two general components of thermo-responsive SMPs, i.e. the switching segment generating the temporary shape and the net points determining the permanent shape are well accepted.<sup>2,16</sup> The net points can either be physical interactions as seen in block copolymers or chemical bonds as seen in thermoset polymers.<sup>2,5</sup> The approaches for thermo-responsive SMPs are block copolymers,<sup>17,18</sup> polymer blends,<sup>19,20</sup> polymer composites,<sup>21</sup> polymer bilayers,<sup>22</sup> etc. Block copolymers have received much attention since they can be prepared in the precise structure to obtain polymer with as-desired  $T_{\text{trans}}$ .

Thermo-responsive triple-SMPs are another class of SMP that contains two  $T_{\text{trans}}$  to enable two temporary shapes. Several triple-SMPs, such as poly( $\epsilon$ -caprolactone)-co-poly(cyclohexyl methacrylate),<sup>14</sup> network of poly( $\omega$ -pentadecalactone) and poly( $\epsilon$ -caprolactone),<sup>23</sup> and liquid crystalline elastomer, namely P5tB-LCN,<sup>24</sup> etc., were reported. It should be noted that in some particular cases, the side chains of copolymer function as the crystalline phase and enroll the soft or hard segment accompanying the polymer backbone. Bellin et al. demonstrated a good example of triple-SMPs, which polyethylene glycol performed as side chains to act as the crystalline phase for random copolymer of two methacrylate terminated polymers, i.e., polycaprolactone and polyethylene glycol.<sup>25</sup> Ahn et al. showed the triple-SMP from random terpolymers containing side chain crystals by ring-opening metathesis polymerization (ROMP) using Grubbs catalyst.<sup>26,27</sup>

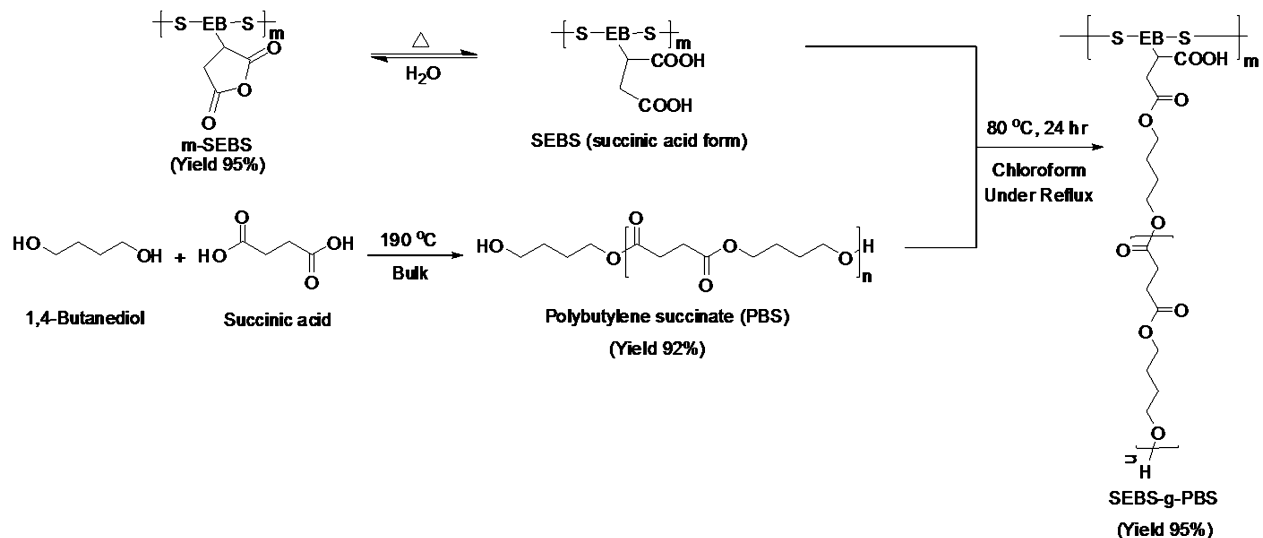
In fact, side chain polymers, in general, can be easily introduced to polymer main chain by “grafting to” technique. However, the “grafting to” to obtain triple-SMPs, to the best of our knowledge, has not yet been reported. The use of grafting is not only attractive in terms of the variety and the ease of the reaction, but also the possibility to develop an inexpensive material with large scale production. It comes to our idea to apply the block copolymer which contains not only hard and

Received: June 8, 2013

Accepted: July 29, 2013

Published: July 29, 2013

Scheme 1. Preparation of SEBS-g-PBS



soft segments to exhibit dual-SME but also the reactive functional groups to be grafted with other hard or soft segment. At that time, the third  $T_{\text{tran}}$  in the polymer chains can be expected. This will lead to a successful “grafting to” as an approach for triple-SMPs.

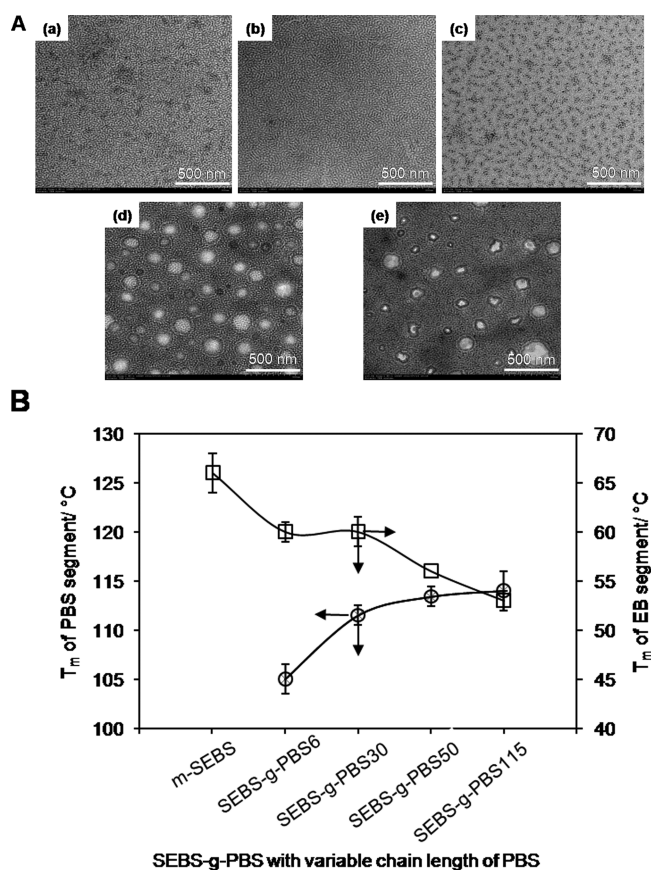
Polystyrene-*b*-poly(ethylene-co-butylene)-*b*-polystyrene triblock copolymer (SEBS) is a good dual-SMP with high shape fixity when it was mixed with paraffin.<sup>28</sup> Maleated-SEBS (m-SEBS) with reactive anhydride group along the SEBS main chain enables us for various modifications.<sup>29</sup>

Poly(butylene succinate) (PBS) is a good candidate of grafting functional group to m-SEBS due to (i) the ease of polycondensation, (ii) the controllable chain lengths based on reaction time, and (iii) the high crystallinity.<sup>30</sup> By simply grafting PBS on m-SEBS, it is expected that we can easily obtain copolymer with side chain crystals (Scheme 1).

## RESULTS AND DISCUSSION

It should be noted that the content of maleic acid for functionalization with PBS is important. The titration with  $\text{CH}_3\text{ONa}$  was carried out to find maleic acid groups for  $1.85 \times 10^{-4}$  mol or 15 units randomly existed in SEBS chains (see the Supporting Information). Separately, four different degree of polymerizations ( $\text{DP}_n$ ) of PBS, i.e., 6 (abbreviated as PBS6), 30 (PBS30), 50 (PBS50), and 115 (PBS115), were prepared (see the Supporting Information, Table S1). The four types of PBS obtained were grafted to m-SEBS to obtain SEBS-g-PBS6, SEBS-g-PBS30, SEBS-g-PBS50, and SEBS-g-PBS115, respectively (see the Supporting Information, Figures S1 and S2, and Table S2).

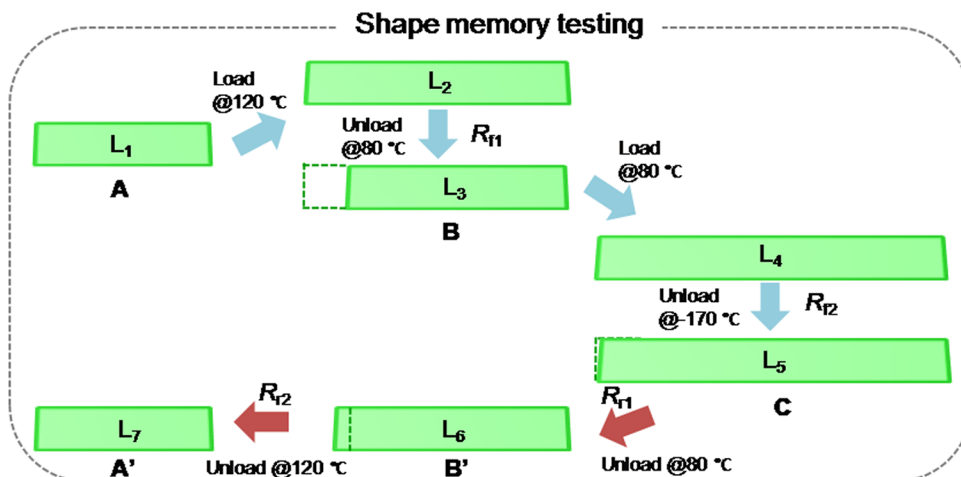
The changes in morphology after grafting of PBS onto m-SEBS were traced. Figure 1A shows transmission electron microscopy (TEM) images of m-SEBS and SEBS-g-PBS after being stained by  $\text{RuO}_4$  and at that time the styrene-rich (S-rich) microdomains show dark images. As m-SEBS has the content of EB for as high as 70%, the PS blocks are found to aggregate as glassy microdomains and embed in the EB matrices. For SEBS-g-PBS, when the chain length of PBS increases, the distances between S-rich microdomains are increased as well. There are some aggregations of PS blocks as evidenced from the dark images (Figure 1A(c)). When the repeat units of PBS are longer, i.e. from 50 to 115, the PS block aggregations become



**Figure 1.** (A) TEM images of (a) m-SEBS, (b) SEBS-g-PBS6, (c) SEBS-g-PBS30, (d) SEBS-g-PBS50, and (e) SEBS-g-PBS115; and (B) two  $T_m$  values of SEBS-g-PBS based on EB segment and PBS segment.

significant until the layer separations are clearly seen (Figures 1A(d, e)). The changes in morphology were relevant to the case of SEBS/paraffin composite reported previously.<sup>28</sup>

It is important to note that all products obtained including m-SEBS show  $T_g$ s of EB and PS segments at approximately  $-50$  °C and  $150$  °C, respectively. SEBS-g-PBS shows two  $T_m$  values belonging to EB and PBS segments (Figure 1B). The  $T_m$  of EB segment decreases in between 65 and 55 °C with an

Table 1. Shape Fixity ( $R_f$ ) and Shape Recovery ( $R_r$ ) of m-SEBS and SEBS-g-PBS

| sample        | $R_{f1}$ (A $\rightarrow$ B) (%) | $R_{f2}$ (B $\rightarrow$ C) (%) | $R_{r1}$ (C $\rightarrow$ B') (%) | $R_{r2}$ (B' $\rightarrow$ A') (%) |
|---------------|----------------------------------|----------------------------------|-----------------------------------|------------------------------------|
| m-SEBS        | 14.6 $\pm$ 1                     | 95.6 $\pm$ 1                     | 97.4 $\pm$ 2                      | 100 $\pm$ 0                        |
| SEBS-g-PBS6   | 80.2 $\pm$ 3                     | 96.4 $\pm$ 1                     | 97 $\pm$ 2                        | 100 $\pm$ 0                        |
| SEBS-g-PBS30  | 83.6 $\pm$ 2                     | 99.2 $\pm$ 1                     | 95.2 $\pm$ 2                      | 99.8 $\pm$ 0                       |
| SEBS-g-PBS50  | 82.8 $\pm$ 2                     | 98.8 $\pm$ 1                     | 94.2 $\pm$ 1                      | 100 $\pm$ 0                        |
| SEBS-g-PBS115 | 85 $\pm$ 3                       | 99 $\pm$ 1                       | 91.8 $\pm$ 2                      | 98.8 $\pm$ 2                       |

increase in PBS chain length. This reflects how the grafted PBS chain obstructs the chain packing of m-SEBS. In contrast,  $T_m$  of PBS segment increases with an increase of PBS chain length from 105 to 115 °C. It is clear that  $T_{trans}$  are varied for  $\sim 10$  °C upon the PBS chain lengths. Here, it should be emphasized that SEBS-g-PBS exhibits two different  $T_m$  values in a single polymer chain, which can be  $T_{trans}$  for triple-SME.

Triple-SMEs were then investigated by cyclic thermomechanical analysis based on the switching domain temperatures, i.e.,  $T_m$  values of EB segment (80 °C) and PBS segment (120 °C). The samples were simply immersed in oil bath at both  $T_m$  values with and without stress to allow fixation and recovery (see Experimental Section in the Supporting Information). Table 1 evaluates the shape memory, of which  $R_f$  represents the ratio of the fixed strain and the maximum strain when the sample was stretched after deformation under  $T_{trans}$  to express the shape fixation and  $R_r$  is for the ratio between the maximum strain and the original shape to determine strain recovery (see the Supporting Information). In the case of m-SEBS, after the sample was heated to 120 °C and cooled down to 80 °C,  $R_{f1}$  is found to be  $\sim 14\%$  meaning that there is some chain fixity. In similar, for SEBS-g-PBS,  $R_{f1}$  is starting from 80% for SEBS-g-PBS6 and increases gradually with increasing PBS chain length. The shape fixity at 80 °C implies the role of PBS, which is the longer the PBS chain length, the higher the crystallization, resulting in the higher shape fixity.<sup>31</sup> It should be noted that  $R_{f2}$ , which referred to the samples after treating at 80 °C and cooling at  $-170$  °C, for all cases is  $\sim 95$ – $99\%$ . This confirms the role of EB segment in fixing the chain.

In term of shape recovery at 80 °C,  $R_{r1}$  (C  $\rightarrow$  B') is  $\sim 95\%$  and decreases with an increase in PBS chain length. It should be noted that shape B' and shape B were almost the same size implying the complete recovery of the sample. The treatment at 80 °C which is below  $T_m$  of PBS might limit the chain mobility to result in an incomplete shape recovery. For  $R_{r2}$ , the recovery for all cases is almost 100% suggesting the free movement of PBS and EB segments above  $T_m$  of PBS (120 °C). The m-SEBS

has two PS end block segments which can form a physical network preventing the chain relaxation<sup>32</sup> at temperature lower than  $T_g$  of PS (150 °C). Thus at 120 °C, the physical network of PS also play an important role on shape recovery.

The triple-SME was also followed by using dynamic mechanical analysis (DMA).  $R_f$  of the products obtained were similar to the results from cyclic thermomechanical analysis. It has to be noted that the  $R_{r2}$   $\sim 88\%$  was obtained after 70 min, which was completely different from what observed in thermomechanical analysis (2 min) (see the Supporting Information, Table S3). In fact, comparing with a sudden immersing the sample in an oil bath at a certain temperature, the time consumed during ramping (heating and cooling) in DMA instrument was much longer and might be enough to allow sample relaxation and creep, which was already described by Fei et al.<sup>33</sup> Therefore, the strain recovery observed by DMA may not directly reflect the actual strain recovery of the sample. However, it should be noted that all evaluation confirmed that SEBS-g-PBS exhibited good shape memory properties.

To discuss the packing structure under the effect of shape fixation, small-angle X-ray scattering (SAXS) was performed. Figure 2 shows 2D SAXS patterns of m-SEBS and SEBS-g-PBS115 in fixation step ( $R_{f1}$  (A  $\rightarrow$  B)). In the case of m-SEBS, the microdomain orientation parallel to the stretching direction (SD) at the original state transforms into an oblique streak pattern upon the fixation process. Considering the fact that, at 80 °C, EB segment can move freely, this might bring the change of lamella orientation during the force application. For SEBS-g-PBS115, the microdomain oriented obliquely to SD is observed for both the original state and after fixation state at 80 °C. This reflects the role of PBS as it crystallized and initiated the packing to obstruct the chain relaxation. The peak width of lamella which becomes wider compared to the original one also informs an increase in crystal phase. The detailed analyses of SAXS patterns of each shape memory step are in our upcoming article.

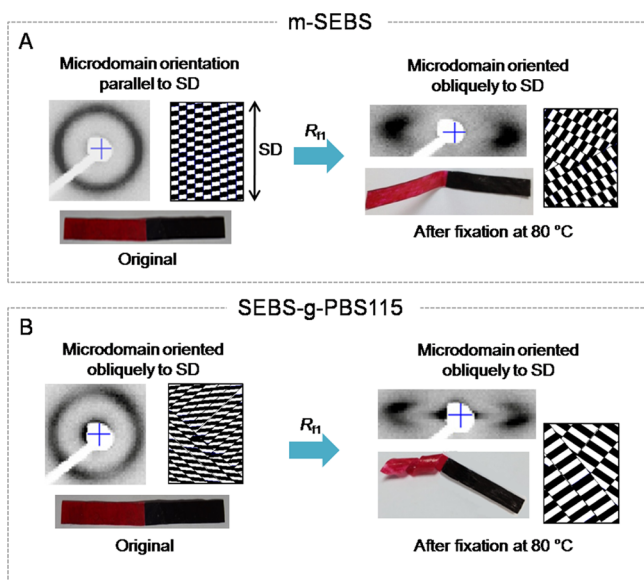


**Figure 2.** SAXS patterns of (A) m-SEBS and (B) SEBS-g-PBS115 during SME.

## CONCLUSIONS

The present work demonstrated an introduction of PBS side chain crystals onto m-SEBS block copolymer backbone as a model case to propose a novel approach of “grafting to” for triple-SMP. Only few percents of PBS grafting lead to drastic changes of m-SEBS for not only the morphologies, thermal behaviors, and rheological properties but also the triple-SME. The  $T_{\text{trans}}$  values belong to the EB segment at  $\sim 55\text{--}65\text{ }^{\circ}\text{C}$ , PBS segment at  $\sim 105\text{--}115\text{ }^{\circ}\text{C}$ , and PS segment at  $\sim 150\text{ }^{\circ}\text{C}$ . The chain length of PBS more or less played the role in shifting the  $T_{\text{trans}}$  of each segment as well as the fixation and recovery efficiency.

## ASSOCIATED CONTENT

### Supporting Information

Methodology to synthesized PBS, m-SEBS, and SEBS-g-PBS; FTIR and NMR spectra of SEBS-g-PBS; DSC curves and mechanical properties of m-SEBS and products obtained; shape memory testing by cyclic thermomechanical analysis and DMA; shape memory video. This material is available free of charge via the Internet at <http://pubs.acs.org>.

## AUTHOR INFORMATION

### Corresponding Author

\*E-mail: [csuwabun@chula.ac.th](mailto:csuwabun@chula.ac.th).

### Notes

The authors declare no competing financial interest.

## ACKNOWLEDGMENTS

The authors express their gratitude to the Thailand Graduate Institute of Science and Technology (TGIST) (Grant TG-33-09-51-049D), the Thailand Graduate Institute of Science and Technology Plus Excellent Center for Eco-Product Development (TGIST Plus XCEP), Prof. Kohji Tashiro for SAXS measurement, and Asahi Kasei Chemical Corporation, Japan for the m-SEBS samples.

## REFERENCES

- (1) Min, C.; Cui, W.; Bei, J.; Wang, S. *Polymer Adv. Technol.* **2005**, *16*, 608–615.
- (2) Lendlein, A.; Kelch, S. *Angew. Chem., Int. Ed.* **2002**, *41*, 2034–2057.
- (3) Hu, J. L.; Ji, F. L.; Wong, Y. W. *Polym. Int.* **2005**, *54*, 600–605.
- (4) Huang, W. M.; Zhao, Y.; Wang, C. C.; Ding, Z.; Purnawali, H.; Tang, C.; Zhang, J. L. *J. Polym. Res.* **2012**, *19*, 9952–9986.
- (5) Behl, M.; Lendlein, A. *Mater. Today* **2007**, *10*, 20–28.
- (6) Sun, L.; Huang, W. M. *Soft Matter* **2010**, *6*, 4403–4406.
- (7) Qi, H. J.; Nguyen, T. D.; Castro, F.; Yakachi, C. M.; Shandas, R. J. *Mech. Phys. Solids* **2008**, *56*, 1730–1751.
- (8) Yu, K.; Xie, T.; Leng, J.; Ding, Y.; Qi, H. J. *Soft Matter* **2012**, *8*, 5687–5695.
- (9) Ge, Q.; Yu, K.; Ding, Y.; Qi, H. J. *Soft Matter* **2012**, *8*, 11098–11105.
- (10) Westbrook, K. K.; Parakh, V.; Chung, T.; Mather, P. T.; Wan, L. C.; Dunn, M. L.; Qi, H. J. *J. Eng. Mater. Technol.* **2010**, *132*, 041011–041019.
- (11) Long, K. N.; Dunn, M. L.; Qi, H. J. *Int. J. Plast.* **2010**, *26*, 603–616.
- (12) Ge, Q.; Luo, X.; Iversen, C. B.; Mather, P. T.; Dunn, M. L.; Qi, H. J. *Soft Matter* **2013**, *9*, 2212–2223.
- (13) Sun, L.; Huang, W. M.; Wang, C. C.; Zhao, Y.; Ding, Z.; Purnawali, H. *J. Polym. Sci. A: Polym. Chem.* **2011**, *49*, 3574–3581.
- (14) Behl, M.; Bellin, I.; Kelch, S.; Wagermaier, W.; Lendlein, A. *Adv. Funct. Mater.* **2009**, *19*, 102–108.
- (15) Wang, C. C.; Huang, W. M.; Ding, Z.; Zhao, Y.; Purnawali, H. *Compos. Sci. Technol.* **2012**, *72*, 1178–1182.
- (16) Wang, W.; Jin, Y.; Ping, P.; Chen, X.; Jing, X.; Su, Z. *Macromolecules* **2010**, *43*, 2942–2947.
- (17) Li, J.; Viveros, J. A.; Wrue, M. H.; Anthanmatten, M. *Adv. Mater.* **2007**, *19*, 2851–2855.
- (18) Xue, L.; Dai, S.; Li, Z. *Biomaterials* **2010**, *31*, 8132–8140.
- (19) Zhang, H.; Wang, H.; Zhong, W.; Du, Q. *Polymer* **2009**, *50*, 1596–1601.
- (20) Ajili, S. H.; Ebrahimi, N. G.; Soleimani, M. *Acta Biomater.* **2009**, *5*, 1519–1530.
- (21) Luo, X.; Mather, P. T. *Macromolecules* **2009**, *42*, 7251–7253.
- (22) Xie, T.; Xiao, X.; Cheng, Y.-T. *Macromol. Rapid Commun.* **2009**, *30*, 1823–1827.
- (23) Zotzmann, J.; Behl, M.; Hofmann, D.; Lendlein, A. *Adv. Mater.* **2010**, *22*, 3424–3429.
- (24) Behl, M.; Lendlein, A. *J. Mater. Chem.* **2010**, *20*, 3335–3345.
- (25) Bellin, I.; Kelch, S.; Lendlein, A. *J. Mater. Chem.* **2007**, *17*, 2885–2891.
- (26) Ahn, S.-K.; Deshmukh, P.; Kasi, R. M. *Macromolecules* **2010**, *43*, 7330–7340.
- (27) Ahn, S.-K.; Kasi, R. M. *Adv. Funct. Mater.* **2011**, *21*, 4543–4549.
- (28) Song, S.; Feng, J.; Wu, P. *Macromol. Rapid Commun.* **2011**, *32*, 1569–1575.
- (29) Liu, Y.; Farinha, J. P. S.; Winnik, M. A. *Macromolecules* **1999**, *32*, 3957–3963.
- (30) Gan, Z.; Abe, H.; Kurokawa, H.; Doi, Y. *Biomacromolecules* **2001**, *2*, 605–613.
- (31) Huang, C.-L.; Jiao, L.; Zhang, J.-J.; Zeng, J.-B.; Yang, K.-K.; Wang, Y.-Z. *Polym. Chem* **2012**, *3*, 800–808.
- (32) Luo, Y.; Guo, Y.; Gao, X.; Li, B.-G.; Xie, T. *Adv. Mater.* **2012**, *25*, 743–748.
- (33) Fei, P.; Cavicchi, K. A. *ACS Appl. Mater. Interfaces* **2010**, *2*, 2797–2803.